Chapter

Investigation of Shielding Effectiveness of M-Type Ba-Co-Ti Hexagonal Ferrite and Composite Materials in Microwave X-Band Systems

Charanjeet Singh, S. Bindra Narang and Ihab A. Abdel-Latif

Abstract

Ferrites are a wide class of materials that are still a very rich field of scientific interest and under the scope of recent research. The polycrystalline Co^{2+}-Ti^{4+} substituted Ba hexagonal ferrite has been synthesized by the standard ceramic method. The vector network analyzer has been incorporated to measure different microwave parameters at X-band (8.2–12.4 GHz) frequencies. The microwave shielding effectiveness is evaluated by S-parameters for near field and AC conductivity as well as skin depth for far field. The doping of Co^{2+} and Ti^{4+} ions causes absorption in composite x = 0.5 to exhibit good shielding effectiveness and it exhibits large 20-dB bandwidth of 4.70 GHz in the near field and 3.60 GHz for far field respectively. The AC conductivity increases with frequency in composites x = 0.1, 0.3, and 0.5 and skin depth decreases with frequency in all composites. The shielding effectiveness, AC conductivity, and skin depth are correlated to each other.

Keywords: ferrites, hexaferrite, microwave shielding, AC conductivity

1. Introduction

Ferrites are a wide class of materials containing iron. These materials are formed in different crystalline symmetries. A simple form of ferrites is the spinel AB_2O_4 of cubic structure [1–9]. The orthoferrites ABO_3 are another important form with an orthorhombic perovskite crystal system [10–19]. The third class of ferrites are garnets of form $A_3B_5O_{12}$ [20–29]. The fourth class, termed as hexaferrites, may be divided into five main groups: M-type ($AB_{12}O_{19}$), W-type ($AMe_2B_{16}O_{27}$), X-type $A_2Me_2B_{28}O_{46}$, Y-type $A_2Me_2B_{12}O_{22}$, and Z-type or $A_3Me_2B_{24}O_{41}$ [30–49]. The preparation of these materials and their characterization are very rich topics because of the wide range of applications and the cheap materials obtained. Ferrites are a very interesting class of materials whose wide range of applications are related to electromagnetic interference suppression as well as their use in radar absorbing material (RAM) coatings [50]. From this point of view, great scientific interests are devoted to use these materials as RAM devices [51–54]. In this work the intensive highlights is devoted to the microwave applications and which class is the best candidate for this application.

The tremendous rise in speed of electronic devices and widespread incorporation of information technology for various technological applications have pumped up electromagnetic pollution to dangerous levels. The high-speed electronic gadgets emit spurious wireless signals rendering the electromagnetic disturbance/interference (EMI) to the electrical and/or electronic circuits in the vicinity.

A microwave absorber reduces unwanted radiation emitted from high-speed electronic devices such as radar, oscillators, and supercomputers. The ferrimagnetic materials ferrites have the potential ability to reduce electromagnetic interference (EMI) in contrast with conventional dielectrics owing to their magneto/dielectric properties [55–60]. Electronic devices constitute integrated circuits (ICs) wherein numerous components are embedded and such components are encapsulated with ferrite films to mitigate EMI. The frequency range of application of extensively used spinel ferrites is limited by Snoek's limit and they are not effective at GHz range. M-type hexagonal ferrites are tailored for EMI diminution in the higher end of microwave region, that is, X-band, Ku-band, K-band, etc. [61–65]: these ferrites allow to tune in the frequency region through doping accompanied by anisotropy field. Both the electric and magnetic properties define the capabilities of these materials to store energy and are described by analyzing the real parts of complex permittivity (ε') and permeability (μ'), respectively. On the other side, imaginary parts (ε'', μ'') are very important parameters that describe the loss of electric and magnetic energy.

Different researches have been devoted to electromagnetic interference (EMI) shielding effectiveness (SE) and EMI shielding mechanisms [66–68] of high structure carbon black (HS-CB)/polypropylene (PP) composites and multiwalled carbon nanotubes-polymethyl methacrylate (MWCNT-PMMA) in the X-band frequency range. They studied different thickness of composite plates electrical conductivities. Their results showed that the absorption loss contribution to the overall attenuation is more than the contribution of the reflection loss for HS-CB/PP composites. Moreover, EMI SE up to 40 dB in the frequency range 8.2–12.4 GHz (X-band) was achieved in Ref. [69] by stacking seven layers of 0.3-mm-thick MWCNT-PMMA composite films compared with 30 dB achieved by stacking two layers of 1.1-mm-thick MWCNT-PMMA bulk composite.

Recently, graphene composites have been found to be one of the most promising candidates for high-performance porous microwave absorbers in ref. [70] because of their 3D conductive network and multiple scattering. A qualified frequency bandwidth (reflection loss <−10 dB) reaches 5.28 GHz covering almost the entire Ku band at 2 mm thickness. These results might open the door for a new design of lightweight coating absorber. This may allow us to say that the performance of microwave devices is mainly based on the properties of the used materials. Knowledge of the frequency dependence of such material is a prerequisite to select suitable materials for various microwave applications and vice versa [71–73]. Novel nanocomposite systems are prepared for microwave applications such as *para*-toluene sulfonic acid (p-TSA)-doped polyaniline (PANI)-graphene nanoplatelet (GRNP) composite films. The addition of GRNPs in the PANI matrix allows to improve the conductivity and dielectric properties of the composites due to the formation of 3D conducting networks. Shielding effectiveness of the PANI-GRNP composite films doped with p-TSA was examined by using S-parameters obtained from vector network analyzer in the X-band microwave frequencies. The efficiency of shielding for these composites depends on GRNP's content in the PANI matrix [74]. Electrical and mechanical properties of carboxylic (–COOH) functionalized multiwall carbon nanotube (MWNTs)/epoxy composites at low wt.% (0.5, 0.75, and 1 wt.%) are studied in Ref. [75]. Microwave shielding effectiveness (SE) for X-band (8–12 GHz) and the flexural properties showed that the total SE of the nanocomposites was increased with the positive gradient of MWNT contents. Great efforts have been made to improve the requirements for microwave

applications in X-band and new materials are being tested [70, 76–78]. Promising results were found and the search for new materials continues.

In the present chapter, we have explored EMI shielding effectiveness characteristics of M-type Ba-Co-Ti hexagonal ferrites.

2. Experimental details

The M-type $BaCo_xTi_xFe_{(12-2x)}O_{19}$ hexaferrites, with x = 0.1, 0.3, 0.5, and 0.7, were prepared by ceramic method. The powder chemicals were mixed thoroughly, ground, and sintered in an electric furnace at 900°C for 7 h. The pellets were made of the powder with the hydraulic press at uniform pressure of 75 kN/m^2 and final sintering was done at 1100°C for 9 h. The crystal structure was measured using Bruker D8Diffractometer of Cu X-ray radiation.

The microwave properties have been studied by the vector network analyzer, Agilent model N5225A. Before performing the measurements, permittivity and permeability of air were measured with an analyzer for calibration purposes. The DC resistivity (ρ_{dc}) was investigated using Keithley Electrometer, model 6514. The selected thickness of composites for optimized characteristics are x = 0.1–3.3 mm, x = 0.3–3.8 mm, x = 0.5–3.4 mm, and x = 0.7–3.2 mm.

3. Results and discussion

Figure 1 shows patterns obtained from X-ray diffraction of $BaCo_xTi_xFe_{(12-2x)}O_{19}$ hexaferrite composites. The observed XRD peaks confirm M-type phase of hexaferrite with space group $P6_3/mmc$. The change of intensity in the peaks shows that the substituted Co^{2+} and Ti^{4+} ions have occupied crystallographic sites.

3.1 Shielding in near field

The shielding effectiveness (SE) is accompanied by reflection or absorption of unwanted microwave signal (EMI) and can be represented as $SE = SE_R + SE_A$ with SE_R due to reflection and SE_A as absorption. When the microwave signal passes

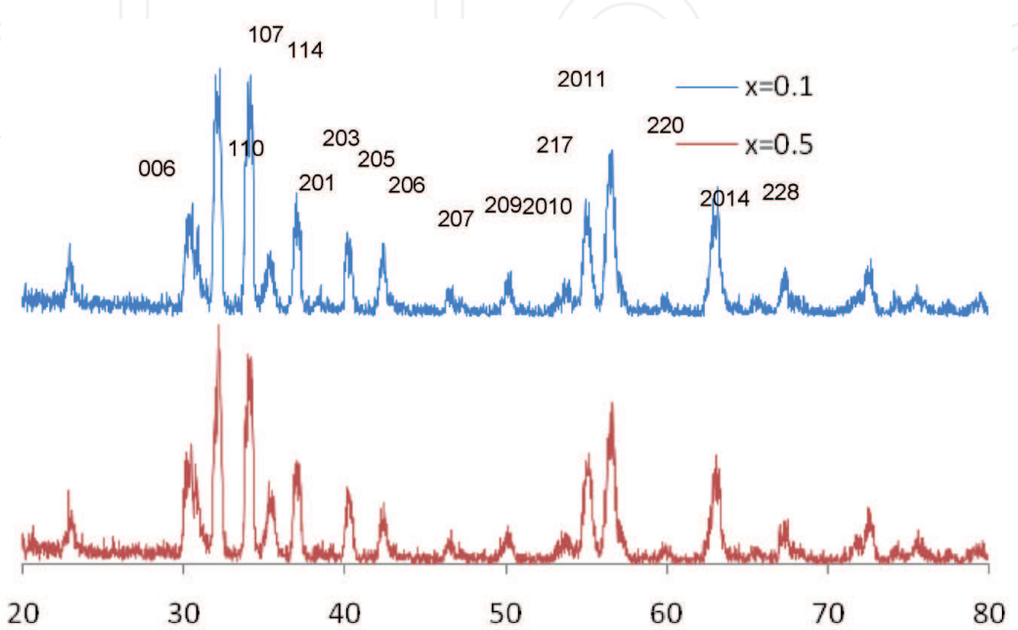

Figure 1.
X- ray diffraction pattern of $BaCo_xTi_xFe_{(12-2x)}O_{19}$ ferrite.

through the material, part of the signal is reflected and remaining transmitted or absorbed. The reflected power (P_r) and transmitted power (P_t) are derived from measured S-parameters: $P_r = |S_{11}|^2$ and $P_t = |S_{22}|^2$, SE_A and SE_R can be calculated as:

$$SE_A = -10\log\left[P_t/(1-P_r)\right] \quad (1)$$

$$SE_R = -10\log(1-P_r) \quad (2)$$

Figure 2 shows plots of EMI shielding effectiveness (SE_A) versus frequency for doping of Co^{2+} and Ti^{4+} ions. Composites x = 0.5 and 0.7 exhibit highest (38.9 dB) and lowest (7.9 dB) values at 10.26 and 12.03 GHz respectively and these composites stay at maximum and minimum values in the frequency regime.

All composites exhibit nonlinear decrease in SE_A with frequency and composites x = 0.1, 0.3, and 0.5 show more dispersion in SE_A with frequency: x = 0.1, 0.3, and 0.7 displaying maxima at 9.27 GHz and x = 0.5 at 10.26 GHz. All composites stay at SE_A > 10 dB or 90% absorption, encompassing the entire frequency region.

Figure 3 depicts the response of shielding effectiveness (SE_R) of $BaCo_xTi_xFe_{(12-2x)}O_{19}$ ferrite versus frequency for doping of Co^{2+} and Ti^{4+} ions. All composites exhibit: (i) minimum SE_R in comparison to SE_A encompassing the entire frequency region, (ii) nearly the same trend of SE_R in the investigated frequency regime, and (iii) maxima in the mid-frequency region. The shielding effectiveness (SE_R) due to reflection is very small and SE_R owe excursion between 0.2 and 2.5 dB. The low SE_R implies no composite can act as a microwave reflector shield. The composite x = 0.5 has largest SE_R = 2.48 dB at 10.39 GHz.

3.2 Shielding in far field

Shielding effectiveness for far field can be evaluated by classical electromagnetic field theory with the following relation [79]:

$$SE(dB) = 10\log(\sigma_{ac}/16\omega\varepsilon_o) + 20(d/\delta)\log e \quad (3)$$

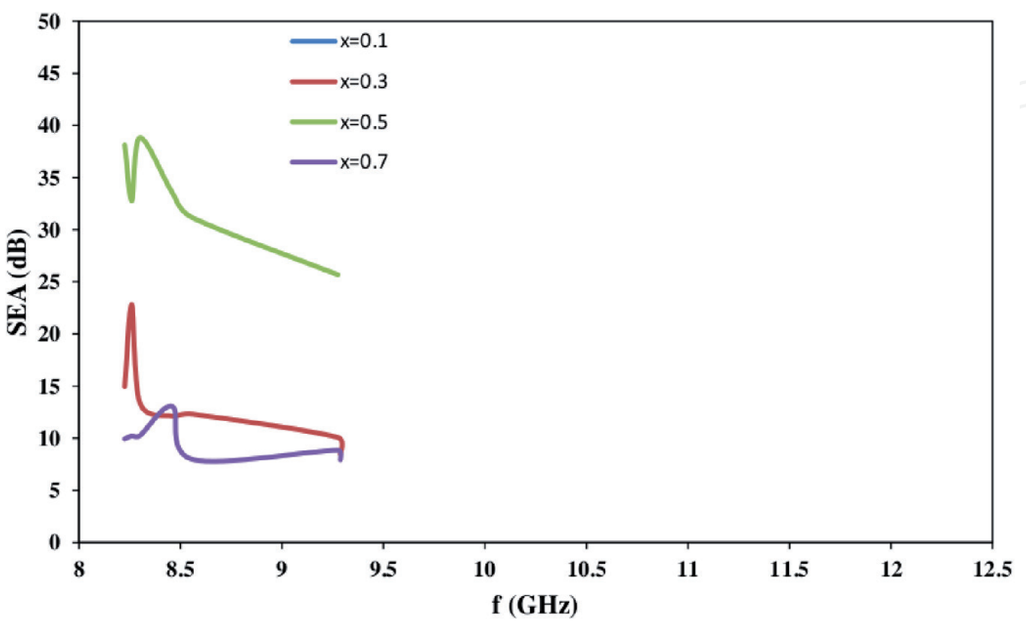

Figure 2.
Variation of shield effectiveness due to absorption (SE_A) with frequency for $BaCo_xTi_xFe_{(12-2x)}O_{19}$ ferrite (x = 0.1, 0.3, 0.5, 0.7).

where σ_{ac} is the AC conductivity, ω is the angular frequency, ε_0 is the absolute permittivity, d is the thickness of the shield, δ is the skin depth, and μ_r is the relative permeability.

Furthermore, $\sigma_{ac} = \omega\varepsilon_0\varepsilon''$ and $\delta = (2/\mu_o\omega\sigma_{ac})^{1/2}$, where μ_o and ε'' are dielectric loss and absolute permeability respectively. The first term, $10\log(\sigma_{ac}/16\omega\varepsilon_0)$, in Eq. (3) is the shielding effectiveness due to reflection and second term, $20(d/\delta)\log e$, relates to the absorption of the microwave signal. The second term is effective at high frequencies and Eq. (3) can be rewritten as:

$$SE_A = 20\,d\left(\mu_o\omega\sigma_{ac}/2\right)^{1/2}\log e \tag{4}$$

Figure 4 depicts the graph of AC conductivity (σ_{ac}) as a function of frequency for doping of Co^{2+} and Ti^{4+}. It increases with doping from x = 0.1, 0.3 and x = 0.5 followed by prevalent fall in x = 0.7: composite x = 0.5 observes more dispersion with frequency and large value of σ_{ac} in comparison to other composites. The rise

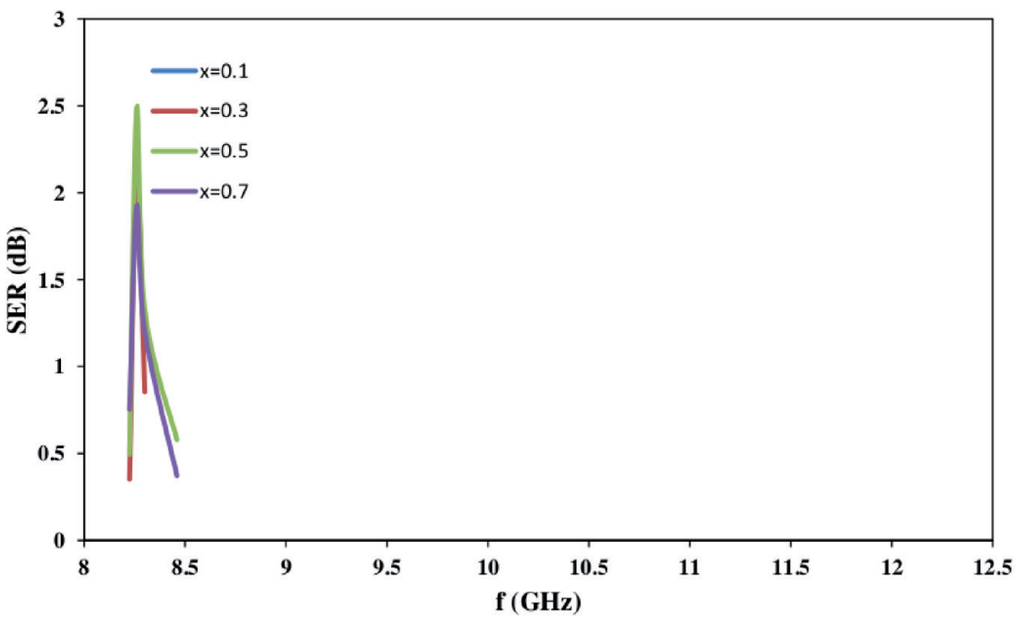

Figure 3.
Variation of shield effectiveness due to reflection (SE_R) with frequency for $BaCo_xTi_xFe_{(12-2x)}O_{19}$ ferrite (x = 0.1, 0.3, 0.5, 0.7).

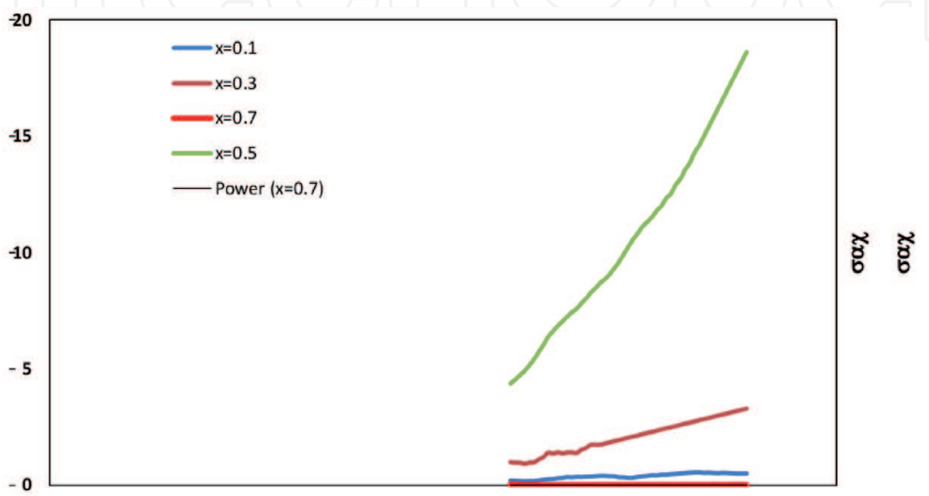

Figure 4.
Plots of AC conductivity versus frequency for $BaCo_xTi_xFe_{(12-2x)}O_{19}$ ferrite (x = 0.1, 0.3, 0.5, 0.7).

in σ_{ac} is seen with frequency in composite x = 0.1, 0.3, and 0.5; however, it remains nearly independent of frequency in x = 0.7. This increase in σ_{ac} is ascribed to Koops-Wagner model, which explains ferrite comprising of heterogeneous structure [80]: ferrites owe layers of good conducting grains, effective at high frequencies, are separated by poor conducting grain boundaries that are effective at low frequencies.

The composites x = 0.1, 0.3, 0.5, and 0.7 have DC resistivity (ρ_{dc}) of 693.6 MΩ cm, 2.8 kΩ cm, 0.5 kΩ cm, and 33.8 MΩ cm, respectively. The composite x = 0.1 has the highest resistivity but still a large σ_{ac} attributed to the presence of more strength of Fe^{3+}: electron hopping between Fe^{3+}–Fe^{2+} ions is responsible for conduction in ferrites [81]. Among all composites, composite x = 0.5 (i) owe maximum σ_{ac} besides with diminution in the number of Fe^{3+} ions and (ii) has the lowest DC resistivity. The competition between these factors altogether increases σ_{ac} in this

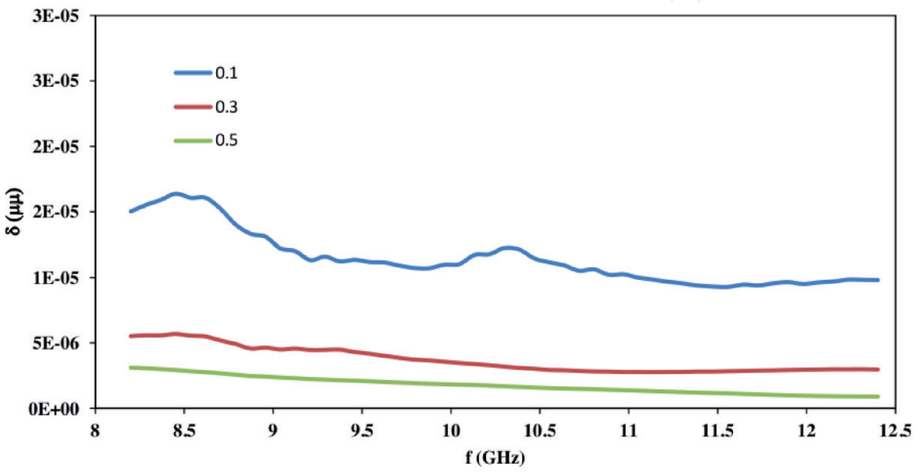

Figure 5.
Change in skin depth (δ) with frequency for $BaCo_xTi_xFe_{(12-2x)}O_{19}$ ferrite (x = 0.1, 0.3, 0.5, 0.7) with frequency in X-band.

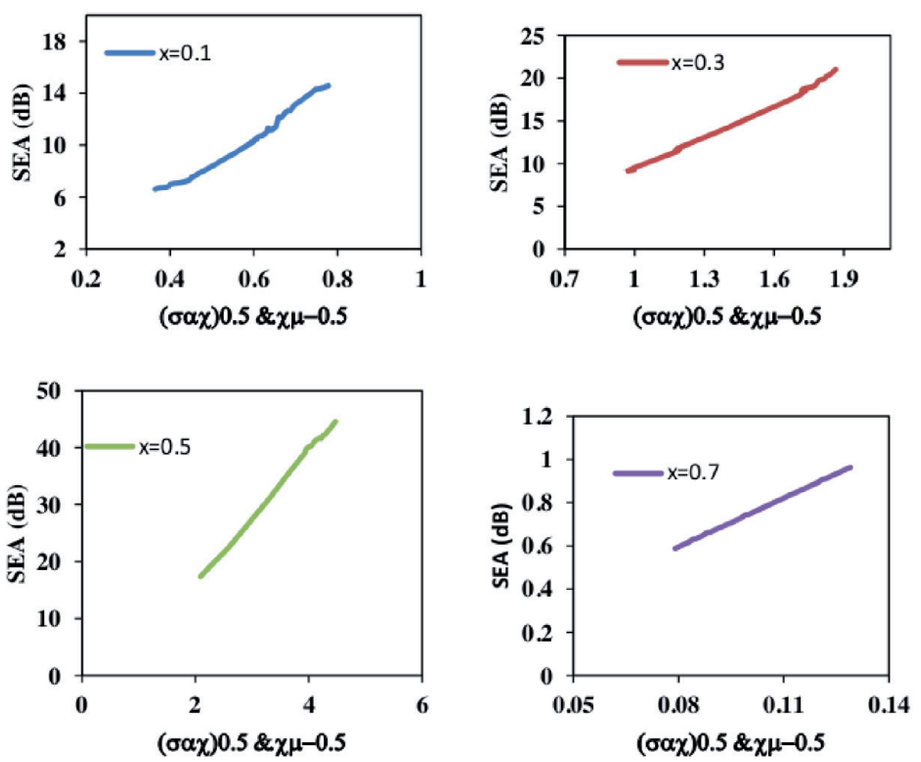

Figure 6.
Plots of SE_A versus $(\sigma_{ac})^{0.5}(S/m)^{0.5}$ for $BaCo_xTi_xFe_{(12-2x)}O_{19}$ ferrite (x = 0.1, 0.3, 0.5, 0.7).

x	Near field				Far field			
	Freq. band (GHz)	10 dB bandwidth (GHz)	Freq. band (GHz)	20 dB bandwidth (GHz)	Freq. band (GHz)	10 dB bandwidth (GHz)	Freq. band (GHz)	20 dB bandwidth (GHz)
0.1	8.26–8.59	0.33	8.59–9.80	1.54	9.20–12.40	3.20	–	–
	9.80–12.03	2.23	–	–	–	–	–	–
0.3	8.26–8.80	0.54	8.80–9.69	0.89	8.70–12.40	3.70	–	–
	9.69–12.03	2.34	–	–	–	–	–	–
0.5	–	–	8.30–11.90	3.60	8.20–8.70	0.50	8.70–12.40	4.70
0.7	8.20–10.32	2.12	–	–	–	–	–	–

Table 1.
Microwave shielding effectiveness (SE_A) for 10- and 20-dB bandwidth (BW) in near and far field in $BaCo_xTi_xFe_{(12-2x)}O_{19}$ (x = 0.1, 0.3, 0.5, 0.7).

composite. Similarly, steep fall of σ_{ac} in x = 0.7 is associated with the least number of Fe^{3+} ions available for electron hopping and large DC resistivity.

The dependence of skin depth (δ) on frequency for a different level of substitution is shown in **Figure 5**. The decrement trend in δ is observed with frequency, and x = 0.7 and 0.5 exhibit large and small δ respectively among the composites in the frequency regime. The large conduction loss, as shown in σ_{ac} (**Figure 4**), causes minimum δ, which attenuates the propagating microwave signal in the composite and vice versa; thus further penetration of signal is not possible inside the thickness of composite: the signal is attenuated more in x = 0.5 due to highest σ_{ac} depicted in **Figure 4**, thereby causing lowest δ.

The dependence of shielding effectiveness (SE_A) on AC conductivity ($\sigma_{ac}{}^{0.5}$) for different levels of doping is shown in **Figure 6**: it increases with doping from x = 0.1 to x = 0.5 and steep decrement is seen thereafter in x = 0.7. All composites display a monotonic trend of increase in SE_A with $\sigma_{ac}{}^{0.5}$ and x = 0.5 owe maximum value while x = 0.7 stay at lowest one.

Table 1 shows bandwidth (10 dB and 20 dB) of SE_A for both near and far field versus doping: 10 and 20 dB means 90% and 99% absorption respectively. For near field, x = 0.1, 0.3, and 0.7 exhibit 10-dB bandwidth of 2.23, 2.34, and 2.12 GHz respectively whereas 20-dB bandwidth of 1.54, 0.89, and 3.60 GHz is observed in x = 0.1, 0.3 and 0.5 respectively. For far field, x = 0.1, 0.3, and 0.5 show 10 dB-bandwidth of 3.20, 3.70, and 0.50 GHz respectively, and 20-dB bandwidth of 4.70 GHz is seen in x = 0.5 only.

4. Conclusions

For near and far field, microwave shielding effectiveness in $BaCo_xTi_xFe_{(12-2x)}O_{19}$ ferrite is governed by absorption and doping of Co^{2+} and Ti^{4+} ion increases SE_A from x = 0.1, 0.3, and 0.5. Composite x = 0.5 owes the highest SE_A of 38.9 dB at 10.26 GHz and 3.4 mm thickness; $\sigma_{ac}{}^{0.5}$, ρ_{dc} and δ are the contributing factors and same composite carries with highest SE_A of 44.6 dB at $\sigma_{ac}{}^{0.5}$ of 4.5 $(Ohm.cm)^{-0.5}$ for far field; s-parameter is the deciding factor. Furthermore, SE_A increases monotonically with frequency and it can be tuned by varying intrinsic and extrinsic parameters. Composite x = 0.5 has far field and near field wideband of 4.70 and 3.60 GHz respectively for 20 dB SE_A. The studied composites have the potential for practical absorber applications. The applications of these composite materials or other composite materials are very an important subject and more research is needed to find the optimum properties and optimum materials for X-band microwave applications.

Acknowledgements

The author *IA Abdel-Latif*, is thankful to the Deanship of Scientific Research in Najran University for their financial support NU/ESCI/16/063 in the frame of the local scientific research program support.

DOI: http://dx.doi.org/10.5772/intechopen.91204

Author details

Charanjeet Singh[1*], S. Bindra Narang[2] and Ihab A. Abdel-Latif[3,4,5*]

1 Department of Electronics and Communication Engineering, Lovely Professional University, Phagwara, Punjab, India

2 Department of Electronics Technology, Guru Nanak Dev University, Amritsar, Punjab, India

3 Physics Department, College of Science and Arts, Najran University, Najran, Kingdom of Saudi Arabia

4 Advanced Materials and Nano-Research Centre, Najran University, Najran, Saudi Arabia

5 Reactor Physics Department, NRC, Atomic Energy Authority, Abou Zabaal, Cairo, Egypt

*Address all correspondence to: rcharanjeet@gmail.com; charanjeet2003@rediffmail.com and ihab_abdellatif@yahoo.co.uk

References

[1] Gismelseed AM, Khalaf KAM, Elzain ME, Widatallah HM, Al-Rawas AD, Yousif AA. The structural and magnetic behavior of the $MgFe_{2-x}CrxO_4$ spinel ferrite. Hyperfine Interactions. 2012. DOI: 10.1007/s10751-011-0529-8

[2] Roumaih K, Manapov RA, Sadykov EK, Pyataev AV. Mossbauer studies of $Cu_{1-x}Ni_xFeMnO_4$ spinel ferrites. Journal of Magnetism and Magnetic Materials. 2005;**288**:267

[3] Abdel Latif IA. Fabrication of nano-size nickel ferrites for gas sensors applications. Journal of Physics. 2012;**1**(2):50-53

[4] Khalaf KA, Al-Rawas A, Gismelseed A, Al-Ruqeishi M, Al-Ani S, Al-Jubouri A, et al. Effects of Zn substitution on structure factors, Debye-Waller factors and related structural properties of the $Mg_{1-x}Zn_xFeNiO_4$ spinels. Advances in Materials. 2019;**8**(2):70-93. DOI: 10.11648/j.am.20190802.15

[5] Maensiri S, Sangmanee M, Wiengmoon A. Magnesium ferrite ($MgFe_2O_4$) nanostructures fabricated by electrospinning. Nanoscale Research Letters. 2009;**4**:221

[6] Fayek MK, Ata-Allah SS. ^{57}Fe Mossbauer and electrical studies of the $(NiO)–(Cr_2O_3)_x–(Fe_2O_3)_{2-x}$ system. Physica Status Solidi A: Applications and Material Science. 2003;**198**(457-464)

[7] Tatarchuk T, Bououdina M, Judith VJ, John Kennedy L. Spinel ferrite nanoparticles: Synthesis, crystal structure, properties, and perspective applications. In: Fesenko O, Yatsenko L, editors. Nanophysics, Nanomaterials, Interface Studies, and Applications. NANO 2016. Springer Proceedings in Physics, vol 195. Springer, Cham. 2017

[8] Zaki HM et al. Synthesis and characterization of nanocrystalline $MgAl_xFe_{2-x}O_4$ ferrites. Journal of Materials Research. 2012;**27**(21):2798

[9] Al-Maashani M, Gismelseed AM, Khalaf KAM, Yousif AA, Al-Rawas AD, Widatallah HM, et al. Structural and Mossbauer study of nanoparticles $CoFe_2O_4$ prepared by sol-gel auto-combustion and subsequent sintering. Hyperfine Interactions. 2018;**239**:15. DOI: 10.1007/s10751-018-1491-5

[10] Yousif AA et al. Study on Mossbauer and magnetic properties of strontium doped neodymium ferrimanganites perovskite-like structure. AIP Conference Proceedings. 2011;**1370**:103

[11] Abdel-Latif IA, Saleh SA. Effect of iron doping on the physical properties of europium Manganites. Journal of Alloys and Compounds. 2012;**530**:116

[12] Bashkirov S et al. Crystal structure, electric and magnetic properties of ferrimanganite $NdFe_xMn_{1-x}O_3$. Izv. RAS, Physical Series. 2003;**67**:1072

[13] Abdel-Latif IA et al. The influence of tilt angle on the CMR in $Sm_{0.6}Sr_{0.4}MnO_3$. Journal of Alloys and Compounds. 2008;**452**:245

[14] Abdel-Latif IA et al. Magnetocaloric effect, electric, and dielectric properties of $Nd_{0.6}Sr_{0.4}Mn_xCo_{1-x}O_3$ composites. Journal of Magnetism and Magnetic Materials. 2018;**457**:126

[15] Bouziane KA et al. Electronic and magnetic properties of $SmFe_{1-x}Mn_xO_3$ orthoferrites (x = 0.1, 0.2 and 0.3). Journal of Applied Physics. 2005;**97**(10A):504

[16] Abdel-Latif IA. Study on the effect of particle size of strontium-ytterbium manganites on some physical properties. AIP Conference Proceedings. 2011;**1370**:108

[17] Parfenov VV, Bashkirov SS, Abdel-Latif IA, Marasinskaya AV. Russian Physics Journal. 2003;**46**:979-983

[18] Ahmed Farag IS et al. Preparation and structural characterization of $Eu_{0.65}Sr_{0.35}Mn_{1-x}Fe_xO_3$. Egyptian Journal of Solids. 2007;**30**(1):149

[19] Abdel-Latif IA. Study on structure, electrical and dielectric properties of $Eu_{0.65}Sr_{0.35}Fe_{0.3}Mn_{0.7}O_3$. IOP Conference Series: Materials Science and Engineering. 2016;**146**:012003

[20] Ding J, Yang H, Miao WF, Mccormick PG, Street R. Journal of Alloys and Compounds. 1995;**221**:70-73

[21] Niaz Akhtar M et al. $Y_3Fe_5O_{12}$ nano particulate garnet ferrites: Comprehensive study on the synthesis and characterization fabricated by various routes. Journal of Magnetism and Magnetic Materials. 2014;**368**:393-400

[22] Yu H, Zeng L, Lu C, Zhang W, Xu G. Materials Characterization. 2011;**62**:378-381

[23] Rastogi AC, Moorthy VN. Materials Science and Engineering. 2002;**B95**:131-136

[24] Sanchez RD, Rivas J, Vaqueiro P, Quintela MAL, Caeiro D. Journal of Magnetism and Magnetic Materials. 2002;**247**:92-98

[25] Liu CP, Li MW, Cui Z, Huang JR, Tian YL, Lin T, et al. Journal of Materials Science. 2007;**42**:6133-6138

[26] Abbas Z, Al-habashi RM, Khalid K, Maarof M. European Journal of Scientific Research. 2009;**36**:154-160

[27] Rajendran M, Deka S, Joy PA, Bhattacharya AK. Journal of Magnetism and Magnetic Materials. 2006;**301**:212-219

[28] Verma S, Pradhan SD, Pasricha R, Sainkar SR, Joy PA. Journal of the American Ceramic Society. 2005;**88**:2597-2259

[29] Aen F, Ahmad M, Rana MU. Current Applied Physics. 2013;**13**:41-46

[30] Singh J et al. Elucidation of phase evolution, microstructural, Mossbauer and magnetic properties of CO_2-Al_3 doped M-type Ba-Sr hexaferrites synthesized by a ceramic method. Journal of Alloys and Compounds. 2017;**695**:1112-1121

[31] Singh C, Narang SB, Hudiara IS, Bai Y, Marina K. Hysteresis analysis of Co–Ti substituted M-type Ba–Sr hexagonal ferrite. Materials Letters. 2009;**63**:1921-1924

[32] Sharbati A, Choopani S, Azar A-M, Senna M. Structure and electromagnetic behavior of nanocrystalline $SrMg_xZr_xFe_{12-2x}O_{19}$ in the 8-12 GHz frequency range. Journal of Solid State Communications. 2010;**150**:2218-2222

[33] Reimann T, Schmidt T, Töpfer J. Phase stability and magnetic properties of $SrFe_{18}O_{27}$ W-type hexagonal ferrite. Journal of the American Ceramic Society. 2019. DOI: 10.1111/jace.16726

[34] Arjunwadkar PR, Salunkhe MY, Dudhe CM. Structural, electrical, and magnetic study of $SrNi^{2+}(Li^{1+}Fe^{3+})_{0.5}Fe_{16}O_{27}$ ferrite. Journal of Solid State Physics. 2013. DOI: 10.1155/2013/471472

[35] Mukhtar A, Grossinger R, Kriegisch M, Kubel F, Rana MU. Characterization of Sr-substituted W-type hexagonal ferrites synthesized by sol–gel autocombustion method. Journal of Magnetism and Magnetic Materials. 2013;**332**:137-145

[36] Meshram MR, Agrawal NK, Sinha B, Misra PS. Journal of Magnetism and Magnetic Materials. 2004;**271**:207

[37] Goldman A. Modern Ferrite Technology. 2nd ed. Springer Publication; 2006. pp. 83

[38] Amer MA, Hemeda OM. Hyperfine Interactions. 1995;**96**:99

[39] Hosaka N et al. Crystal structure and magnetic properties of X-type hexagonal ferrite $Ba_2Ni_2Fe_{28}O_{46}$. Journal of the Japan Society of Powder and Powder Metallurgy. 2010;**57**:41-45

[40] Gu BX. Magnetic properties of *X*-type $Ba_2Me_2Fe_{28}O_{46}$ (Me = Fe, Co, and Mn) hexagonal ferrites. Journal of Applied Physics. 1992;**71**:5103. DOI: 10.1063/1.350613

[41] Gu BX. Magnetic properties of $Ba_2Me_2Fe_{28}O_{46}$ (Me_2-*X*, Me = Ni, Cu, Mg, and Zn) hexaferrites. Journal of Applied Physics. 1991;**70**:372. DOI: 10.1063/1.350284

[42] Ben-Xi G, Huai-Xian LU, You-Wei DU. Magnetic properties and Mössbauer spectra of X type hexagonal ferrites. Journal of Magnetism and Magnetic Materials. 1983;**31-34**(Part 2):803-804

[43] Reddy MB, Reddy PV. Low-frequency dielectric behaviour of mixed Li-Ti ferrites. Journal of Physics D: Applied Physics. 1991;**24**:975

[44] Bayrakdar H. Fabrication, magnetic and microwave absorbing properties of $Ba_2Co_2Cr_2Fe_{12}O_{22}$ hexagonal ferrites. Journal of Alloys and Compounds. 2016;**675**:185-188

[45] Bai Y, Zhou J, Gui Z, Yue Z, Li L. Complex Y-type hexagonal ferrites: An ideal material for high-frequency chip magnetic components. Journal of Magnetism and Magnetic Materials. 2003;**264**(1):44-49

[46] Lee SG, Kwon SJ. Saturation magnetizations and Curie temperatures of Co-Zn Y-type ferrites. Journal of Magnetism and Magnetic Materials. 1996;**153**:279-284

[47] Smit J, Wijn HPJ. Ferrites. Eindhoven, The Netherlands: Philips Technical Library; 1965. p. 177

[48] Sugimoto M. In: Wohlfarth EP, editor. Ferromagnetic Materials. Vol. 3. Amsterdam: North-Holland; 1982. p. 393

[49] Lubitz P, Rachford FJ. Z type Ba hexagonal ferrites with tailored microwave properties. Journal of Applied Physics. 2002;**91**:7613. DOI: 10.1063/1.1453932

[50] Nakamura T, Hankui E. Control of high-frequency permeability in polycrystalline (Ba,Co)-Z-type hexagonal ferrite. Journal of Magnetism and Magnetic Materials. 2003;**257**(2-3):158-164

[51] Narang SB, Kaur P, Bahel S, Singh C. Microwave characterization of Co–Ti substituted barium hexagonal ferrites in X-band. Journal of Magnetism and Magnetic Materials. 2016;**405**:17-21

[52] Zhang BS, Feng Y, Xiong J, Yang Y, Lu HX. Microwave-absorbing properties of de-aggregated flake-shaped carbonyl-iron particle composites at 2-18GHz. IEEE Transactions on Magnetics. 2006;**42**:1778-1781

[53] Singh P, Babbar VK, Razdan A, Srivastava SL, Puri RK. Complex permeability and permittivity, and microwave absorption studies of $Ca(CoTi)_xFe_{12-2x}O_{19}$ hexaferrite composites in X-band microwave frequencies. Materials Science and Engineering. 1999;**B67**:132-138

[54] Sugimoto S, Haga K, Kagotani T, Inomata K. Microwave absorption properties of BaM-type ferrite prepared by a modified co precipitation method. Journal of Magnetism and Magnetic Materials. 2005;**290**:1188-1191

[55] Singh C, Narang SB, Hudiara IS, Sudheendran K, James Raju KC. Complex permittivity and complex permeability of Sr ions substituted Ba ferrite at X-band. Journal of Magnetism and Magnetic Materials. 2008;**3**(20):1657-1665

[56] Lima UR, Nasar MC, Rezende MC, Araugo JH. Journal of Magnetism and Magnetic Materials. 2008;**320**:1666

[57] Aphesteguy JC, Pamiani A, Digiovanni D, Jacobo SE. Physica B. 2009;**404**:2713

[58] Huang X, Zhang J, Lai M, Sang T. Journal of Alloys and Compounds. 2015;**627**:367

[59] Koledintseva MY, Mikhailovsky LK, Kitaytsev AA. IEEE Transactions on Electromagnetic Compatibility. 2000;**2**:773

[60] Meng P, Xiong K, Ju K, Li S, Xu G. Journal of Magnetism and Magnetic Materials. 2015;**385**:407

[61] Liu J, Zhang J, Zhang P, Wang S, Lu C, Li Y, et al. Materials Letters. 2015;**158**:53

[62] Meng P, Xiong K, Wang L, Li S, Cheng Y, Xu G. Journal of Alloys and Compounds. 2015;**628**:75

[63] Singh C, Bindra Narang S, Vikramjit Singh, Kotnala RK. IEEE 15th International Symposium on Antenna Technology and Applied Electromagnetics (ANTEM), Toulouse; 2012

[64] Singh C, Bindra Narang S, Hudiara IS. IEEE XXX General Assembly and Scientific Symposium of the International Union of Radio Science (URSI), Istanbul; 2011

[65] Singh C, Bindra Narang S, Hudiara IS, Koledintseva MY, Kitaitsev AA. Asia-Pacific Radio Science Conference (AP-RASC'10) Toyama. Paper E4-3; 2010

[66] Al-Saleh MH, Sundararaj U. X-band EMI shielding mechanisms and shielding effectiveness of high structure carbon black/polypropylene composites. Journal of Physics D: Applied Physics. 2012;**46**(3):035304

[67] Cui R-B, Zhang C, Zhang J-Y, Xue W, Hou Z-L. Highly dispersive GO-based supramolecular absorber: Chemical-reduction optimization for impedance matching. Journal of Alloys and Compounds. 2020;**155122**

[68] Raveendran A, Sebastian MT, Raman S. Applications of microwave materials: A review. Journal of Electronic Materials. 2019;**48**(5):2601-2634

[69] Pande S, Singh BP, Mathur RB, Dhami TL, Saini P, Dhawan SK. Improved electromagnetic interference shielding properties of MWCNT? PMMA composites using layered structures. Nanoscale Research Letters. 2009;**4**(4):327-334

[70] Kashi S, Hadigheh SA, Varley R. Microwave attenuation of graphene modified thermoplastic poly (butylene adipate-co-terephthalate) nanocomposites. Polymers. 2018;**10**(6):582

[71] Abdel-Latif IA. Crystal structure and electrical transport of nano-crystalline strontium-doped neodymium ortho-ferrites. Journal of Nanoparticle Research. 2020;**22**:60

[72] Saleh S, Abdel-Latif I, Hakeem AA, et al. Structural and frequency-dependent dielectric properties of $(SnO_2)_{1-x}$ $(Fe_2O_3)_x$. Journal of Nanoparticle Research. 2020;**22**:44. DOI: 10.1007/s11051-020-4763-3

[73] Abdel-Latif IA. The particle size effect of $Yb_{0.8}R_{0.2}MnO_3$ (R is

Sm, Nd, and Eu) on some physical properties. Journal of Nanoparticle Research. 2020;**22**:45. DOI: 10.1007/s11051-020-4759-z

[74] Khasim S. Polyaniline-graphene nanoplatelet composite films with improved conductivity for high performance X-band microwave shielding applications. Results in Physics. 2019;**12**:1073-1081

[75] Bal S, Saha S. Scheming of microwave shielding effectiveness for X band considering functionalized MWNTs/epoxy composites. IOP Conference Series: Materials Science and Engineering. 2016;**115**(1):012027

[76] Arora M, Wahab MA, Saini P. Permittivity and electromagnetic interference shielding investigations of activated charcoal loaded acrylic coating compositions. Journal of Polymers. 2014

[77] Das NC, Chaki TK, Khastgir D, Chakraborty A. Electromagnetic interference shielding effectiveness of conductive carbon black and carbon fiber‐filled composites based on rubber and rubber blends. Advances in Polymer Technology: Journal of the Polymer Processing Institute. 2001;**20**(3):226-236

[78] Das NC, Chaki TK, Khastgir D, Chakraborty A. Electromagnetic interference shielding effectiveness of ethylene vinyl acetate based conductive composites containing carbon fillers. Journal of Applied Polymer Science. 2001;**80**(10):1601-1608

[79] Colaneri NF, Shacklette LW. IEEE Transactions on Instrumentation and Measurement. 1992;**41**:291

[80] Maxwell JC. New York: Oxford University Press; 2004. p. 828

[81] Van Uitert LG. The Journal of Chemical Physics. 1955;**23**:1883